

# Acetylene hydrogenation on anatase $\text{TiO}_2(101)$ supported $\text{Pd}_4$ cluster: oxygen deficiency effect

Jie Yang · Li-Xin Cao · Gui-Chang Wang

Received: 29 October 2011 / Accepted: 16 December 2011 / Published online: 20 January 2012  
© Springer-Verlag 2012

**Abstract** Acetylene hydrogenation on both the perfect and oxygen defective anatase  $\text{TiO}_2(101)$  surfaces supported  $\text{Pd}_4$  cluster has been studied using density functional theory calculations with a Hubbard U correction (DFT + U). The adsorbed  $\text{Pd}_4$  cluster on the perfect surface prefers to form a tetrahedral structure, while it likely moves to the oxygen defective site to form a distorted tetrahedral structure by removing a bridging oxygen atom. For the defective surface, it exhibits a stronger ability to capture  $\text{Pd}_4$  cluster as charge transfer is significantly performed due to the oxygen deficiency. Moreover, it is found that the oxygen defective surface shows higher activity for acetylene hydrogenation, and the possible reason may lie in the weaker adsorption strength between the Pd cluster and the adsorbed molecules on the defective surface as compared to the case on the perfect surface.

**Keywords** Acetylene selective hydrogenation · Anatase · DFT+U · Oxygen deficiency ·  $\text{Pd}_4$  cluster

## Introduction

The industrial manufacture of high-purity ethylene prepared by oil cracking often contains trace amount of acetylene, which results in ethylene loss and catalyst poisoning [1, 2]. Removal of acetylene demands highly optimized catalysts, which are selective to ethylene and opposed to further hydrogenation to ethane.

Titanium dioxide is a preferred system recently used industrially. Because it is not only a promising catalyst in heterogeneous catalysis but also exhibits better photoelectric and photochemical characters, which brings a wide range of applications in improving materials and catalysts in many fields [3–5]. As many growth studies of small metals on titania are studied, it is found that titania is not merely a structural support, but an efficient support, which shows metal-support interaction in hydrogenation reactions. After noble metal supported on reducible  $\text{TiO}_2$ , it will manifest superior catalytic performance in hydrogenation reactions for the interaction effect. Among them, the Pd-TiO<sub>2</sub> catalysts have received particular interest in acetylene hydrogenation [6, 7].

As titanium dioxide contains three main crystal phases: anatase, rutile, brookite, and among them the anatase titania has been extensively investigated for its superior photocatalytic activity possessing a relative wider band gap energy than the rutile phase. Thus, anatase titania is considered to be more active than rutile [8]. By electron paramagnetic resonance (EPR) and infrared spectrum (IR) approaches Li et al. [9] showed that anatase titania supported palladium catalyst performed strong metal-support interaction (SMSI) effect at low temperature but not for rutile one. The SMSI effect was caused by the  $\text{Ti}^{3+}$  ions, which was produced by reduction of  $\text{Ti}^{4+}$  in the surface lattice of anatase titania (*i.e.*, the oxygen defect anatase). However, it was difficult for rutile titania, which was more thermodynamically and structurally

J. Yang · G.-C. Wang  
Department of Chemistry and the Center of Theoretical Chemistry,  
Nankai University,  
Tianjin 300071, People's Republic of China

L.-X. Cao  
Department of Food and Chemistry, Henan Quality Polytechnic,  
Ping Dingshan 467000, People's Republic of China

G.-C. Wang (✉)  
College of Chemistry and Chemical Engineering,  
Shanxi Datong University,  
Datong 037009, Shanxi Province, People's Republic of China  
e-mail: wangguichang@nankai.edu.cn

stable than anatase titania. Panpranot et al. [6] hold the opinion that the presence of  $\text{Ti}^{3+}$  ions in contact with Pd can probably lower the adsorption strength of ethylene, thus increasing ethylene gain. Namely, using pure anatase titania that contained  $\text{Ti}^{3+}$  as supports for Pd catalysts gave high ethylene selectivity. Xu et al. [10] used scanning tunneling microscopy and observed the adsorption of palladium on the  $\text{TiO}_2(110)$  surface in the form of dimer and tetramer Pd clusters. And Zhang et al. [11] studied the growth of palladium clusters supported on anatase  $\text{TiO}_2(101)$  surface and found the number of Pd atoms reached four, which will construct a three-dimensional structure. Thus the three-dimensional structure of  $\text{Pd}_4$  cluster is used to explore its interaction with the supporting anatase titania surfaces.

Therefore, we select stable structures to support  $\text{Pd}_4$  cluster on both the perfect and oxygen defective anatase  $\text{TiO}_2(101)$  surfaces. By DFT+U calculations, the results of the acetylene hydrogenation on the two catalysts can be very useful in understanding the interaction between the adsorbate and support. Besides, our knowledge about electronic structure of its point defect is relatively poor and whether  $\text{Ti}^{3+}$  plays an important role also need to be illustrated clearly. Therefore, to assess the different adsorption behaviors of acetylene, ethylene and other intermediates on both the perfect and oxygen defective anatase (101) surfaces, it will shed light on the effect of oxygen deficiency on the subsequent reactivity of the reaction. And d-band states and charge analysis will provide significant insight into the interaction between the adsorbate and surface.

## Calculation method and models

To study the energy and structure details of acetylene hydrogenation on anatase surfaces, the periodic, self-consistent DFT calculations were performed by using the Vienna *ab initio* simulation package (VASP) [12, 13]. The electronic structures were calculated using DFT within the generalized gradient approximation (GGA-PW91) [14]. The project-augment wave (PAW) [15, 16] scheme was used to describe the inner cores, and the electronic wave functions were expended in a plane wave basis with the kinetic cut-off energy of 400 eV. As conventional DFT calculations based on the local density approximation (LDA) and GGA significantly underestimate the band gap of titania, an additional term U is used to analyze electron correlations in transition metal oxides and express the repulsion between electrons placed on the same orbital. In our GGA+U calculations, the value of U parameter was determined to be 4.0 eV for the Ti atom [17–21]. Transition state (TS) was determined in the following three steps: first, nudged elastic band (NEB) [22] method was employed to locate the likely transition states; second, the likely transition states were relaxed using a quasi-Newton algorithm to make the forces on

the atoms less than 0.05 eV/Å; and lastly, the frequency analysis was performed to be a confirmation of the transition state structures.

In the calculation, the lattice constant is obtained by optimization from the reported experimental value. As a result, optimized lattice constant of bulk anatase  $\text{TiO}_2$  structure ( $a=3.80$  Å,  $c=9.60$  Å,  $c/a=2.53$ ) is in good agreement with the experimental value of  $c=9.50$  Å [3]. This identified the validity of parameters setting in our work. Symmetric periodic slab model is selected for the anatase structure. By cleaving the bulk in the (101) directions, thus we obtain  $10.33 \times 11.41$  Å surface unit cell. The model includes  $1 \times 3$  sized  $\text{TiO}_2$  (101) substrate of 12 atomic layers, containing four Ti atomic layers and eight O atomic layers. The slabs are set at a vacuum region of 15 Å. During the optimization, the six uppermost layers are allowed to fully relax. The oxygen defect surface is made by removing one oxygen atom from the “bridging oxygen” rows protruded from the surface plane on relaxed anatase  $\text{TiO}_2(101)$  surface, which is twofold-coordinated, namely  $\text{O}_{2\text{C}}$ . It bonds with both the nearer sixfold-coordinated titania atoms ( $\text{Ti}_{6\text{C}}$ ) and the fivefold-coordinated titania atoms ( $\text{Ti}_{5\text{C}}$ ). The “bridging oxygen” rows are less stable and can easily be reduced, thus we determined to analyze the nature of such oxygen vacancy in the bulk of the anatase polymorph of titania by means of DFT+U calculations. The perfect anatase is modeled with 72 atoms, including 24 Ti atoms and 48 O atoms. While the defect surface is modeled with 71 atoms including 47 O atoms. The difference of oxygen atom is labeled with the black ball in the top (Fig. 1a) and side (Fig. 1b) views of the anatase surface. The unit cell with the defective oxygen (Ov) concentration is 1/24 per Ti atom. The k-point ( $2 \times 2 \times 1$ ) is selected [23] and the stable structures of acetylene, ethylene, ethane and possible intermediates are discussed. Also, the results of test calculations for cutoff energy of 450 eV and k-point of  $3 \times 3 \times 1$  are calculated and the energy differences are less than 0.01 eV. Therefore, the convergence criteria used in this study is enough and the same as those in the previous study [18, 19]. Adsorption energy ( $E_{\text{ads}}$ ) and the activation energy ( $E_a$ ) are also calculated by the following formulas:  $E_{\text{ads}} = E_{\text{A/M}} - E_{\text{A}} - E_{\text{M}}$  and  $E_a = E_{\text{TS}} - E_{\text{IS}}$ , where  $E_{\text{A}}$ ,  $E_{\text{M}}$ ,  $E_{\text{A/M}}$ ,  $E_{\text{TS}}$  and  $E_{\text{IS}}$  represent the energies of the adsorbate, substrate, coadsorption, TS and IS (initial state).

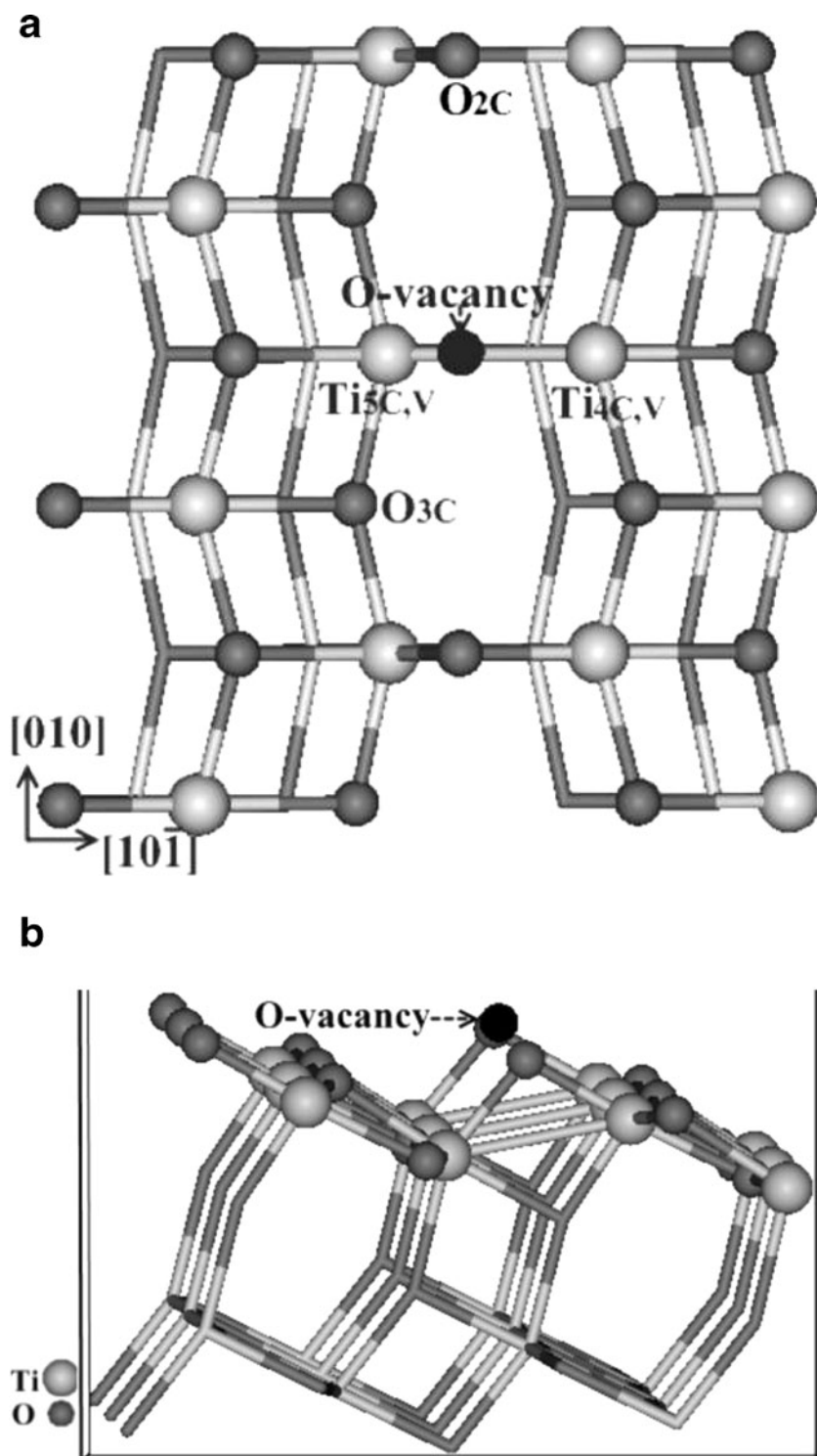
## Results and discussion

Adsorption properties of possible species on anatase  $\text{TiO}_2(101)$  surface

### Perfect and defective anatase $\text{TiO}_2(101)$

The perfect anatase (101) surface has a stepped structure along the [010] direction with the “bridging oxygen” row

**Fig. 1** Top view (a) and side view (b) of the anatase  $\text{TiO}_2(101)$  surface; the black ball signs the  $\text{O}_{2\text{C}}$  site



protruding from the surface plane, which is twofold-coordinated, namely  $\text{O}_{2\text{C}}$ . For perfect anatase (101) surface, the sixfold-coordinated titania atoms ( $\text{Ti}_6\text{C}$ ), fivefold-coordinated titania atoms ( $\text{Ti}_5\text{C}$ ) and threefold-coordinated oxygen atoms ( $\text{O}_{3\text{C}}$ ) are exposed; among them the  $\text{O}_{2\text{C}}$  and  $\text{Ti}_5\text{C}$  atoms are unsaturated. By removing one oxygen atom from the system, unsaturated fivefold-coordinated titania

atoms ( $\text{Ti}_{5\text{C},\text{V}}$ ) and fourfold-coordinated titania atoms ( $\text{Ti}_{4\text{C},\text{V}}$ ) are gained in oxygen defective anatase (101) surface. The oxygen defective formation energy ( $E_{\text{f}}(\text{O})$ ) of the two kinds of oxygen atoms ( $\text{O}_{2\text{C}}$  and  $\text{O}_{3\text{C}}$ ) on the surface are defined by the following equation:

$$E_{\text{f}}(\text{O}) = E_{\text{def}} - E_{\text{free}} + 1/2 E_{\text{o}_2}, \quad (1)$$

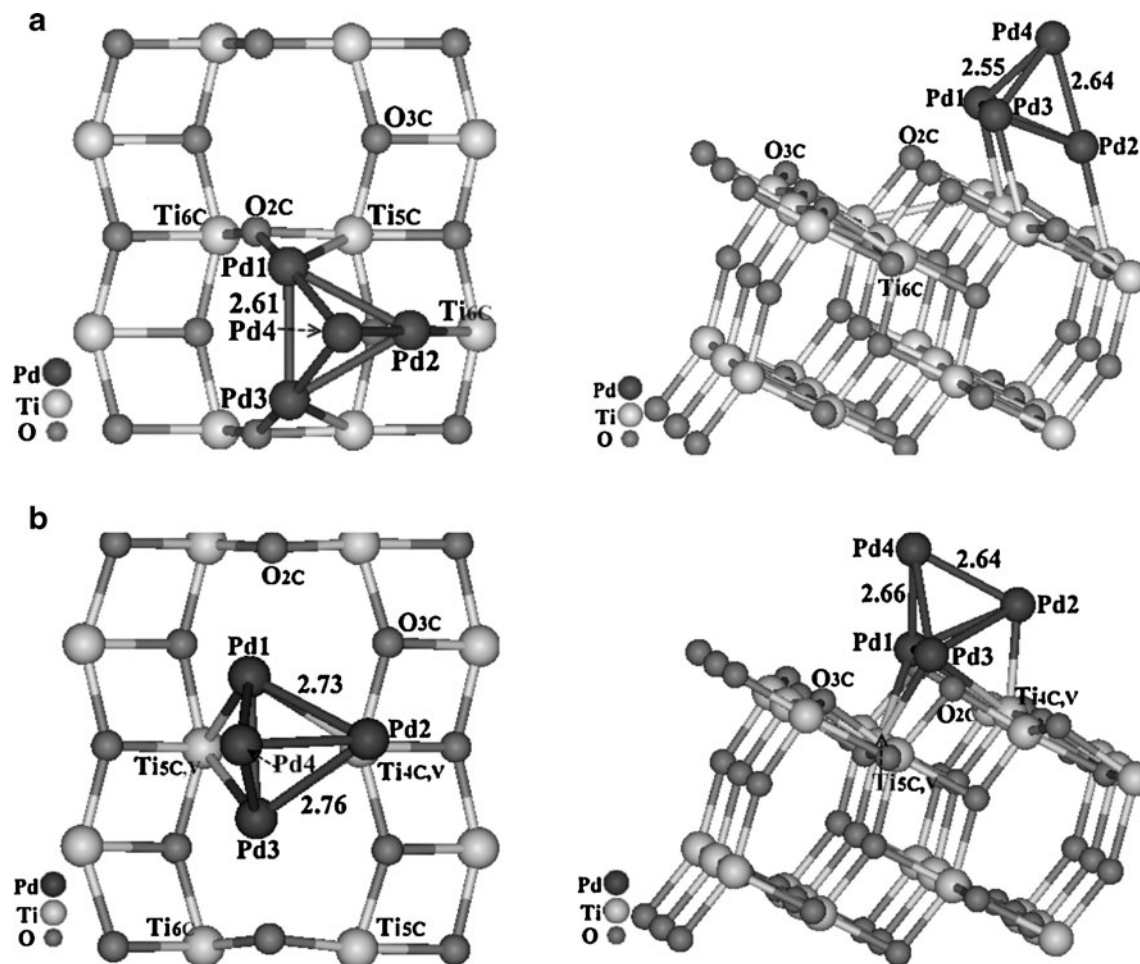


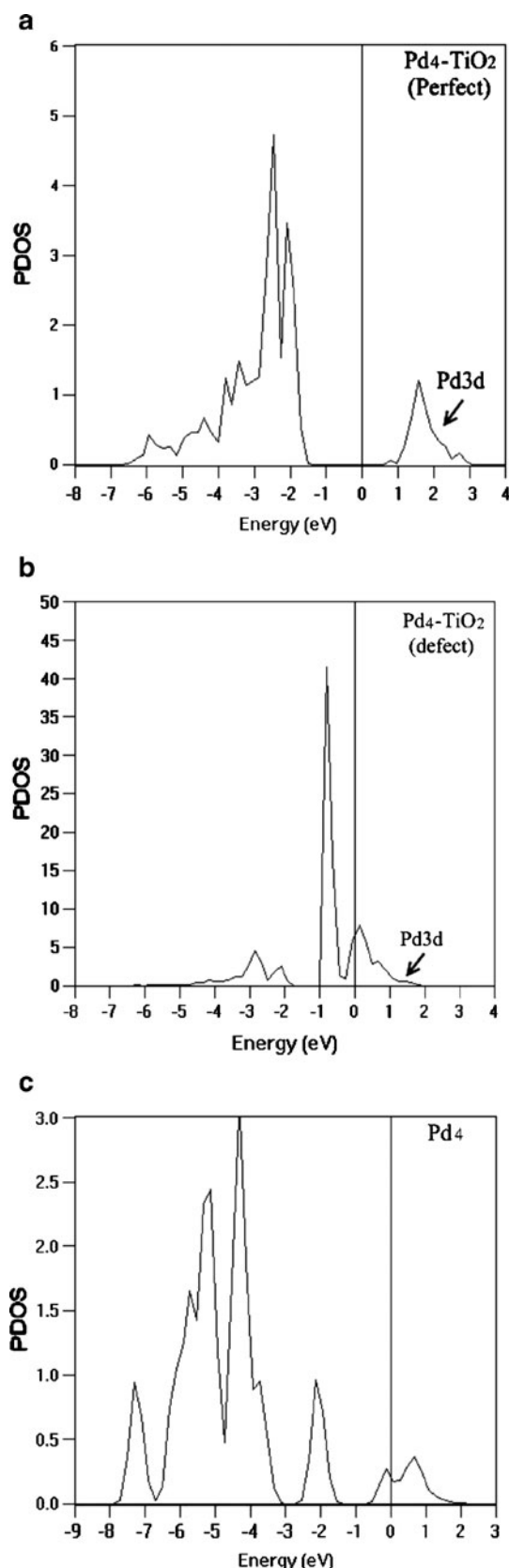
**Fig. 2** Top view and side view of the most stable structures of  $\text{Pd}_4$  cluster adsorbed on the perfect (a) and defective (b) anatase  $\text{TiO}_2(101)$  surfaces. Bond lengths are in Å

where  $E_{\text{def}}$ ,  $E_{\text{free}}$  and  $E_{\text{O}_2}$  are the energies of the defect system, the perfect system and the free molecular oxygen. All the vacancy formation is an endoenergetic process with the defect formation energies of 559.61 and 615.57  $\text{kJ mol}^{-1}$  for  $\text{O}_{2\text{C}}$  and  $\text{O}_{3\text{C}}$ . By comparison, the lattice oxygen of  $\text{O}_{3\text{C}}$  is more stable and tightly bonded than  $\text{O}_{2\text{C}}$ . Thus, the neighboring Ti atoms around  $\text{O}_{2\text{C}}$  are reduced.

#### $\text{Pd}_4$ cluster adsorption on perfect and defective anatase $\text{TiO}_2(101)$ surfaces

Two possible structures for  $\text{Pd}_4$  clusters: a tetrahedral in  $\text{T}_d$  symmetry [24] and a planar in  $\text{D}_{2\text{h}}$  symmetry [25, 26] adsorbed on both perfect and defective titania surfaces are calculated. Comparing the adsorption energies of the two  $\text{Pd}_4$  structures, the most stable structure is a tetrahedral configuration consistent with the previous calculations on  $\text{Pd}_4$  cluster [27]; and its Pd–Pd bonds are formed with an average length of 2.61 Å, in agreement with the result by Valero et al. [28]. When it was deposited on the  $\text{TiO}_2$  surfaces, its geometry was

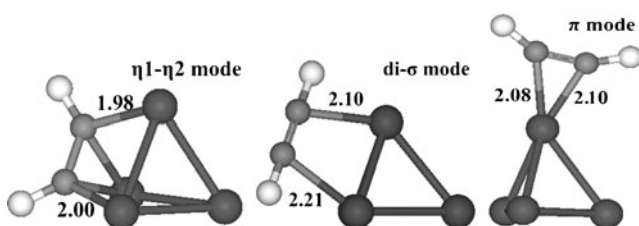
fully optimized with the distorted tetrahedral structures, and their adsorption energies on the perfect and defect anatase surfaces are  $-232.53$  and  $-437.08 \text{ kJ mol}^{-1}$ . For perfect anatase surface, the Pd1 and Pd3 atoms almost locate at the top site of the two  $\text{O}_{2\text{C}}$  atoms while the Pd2 atom bridges between the  $\text{O}_{3\text{C}}$  and  $\text{Ti}_{6\text{C}}$ . The Pd4 atom is at the top site of the triangle geometry constructed by the three Pd atoms. And the Pd–Pd bonds with an average length of 2.63 Å are formed after adsorption on the perfect surface. After removal of the bridging oxygen atom, the tetrahedral structure preferably moves to the oxygen defective site ( $\text{O}_V$ ) to form the distorted tetrahedral structures (see in Fig. 2), with higher adsorption strength. Sanz et al. [26] adopted the DFT calculations and pointed out the adsorption strength of Pd atoms at oxygen defective surface was stronger than that at perfect surface, for the polarization of Pd atoms. Thus, oxygen deficiency is more likely to induce interaction with  $\text{Pd}_4$  cluster. Also the Pd–Pd distances are formed on the defect surface with an average length of 2.69 Å. In both cases, the tetrahedral structures are slightly distorted on the  $\text{TiO}_2$  surfaces with elongated Pd–Pd bond



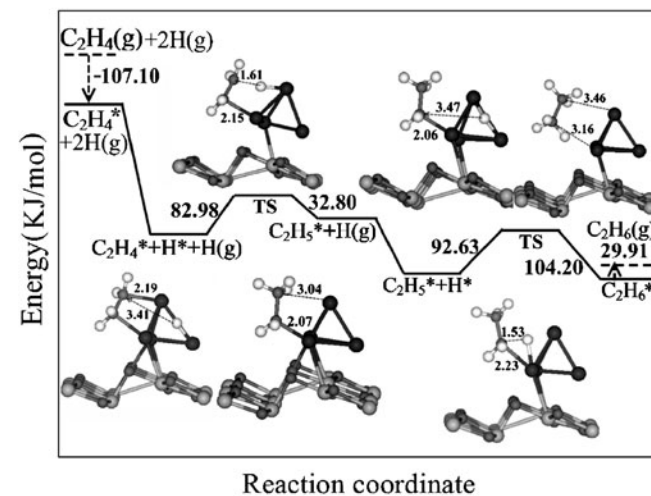
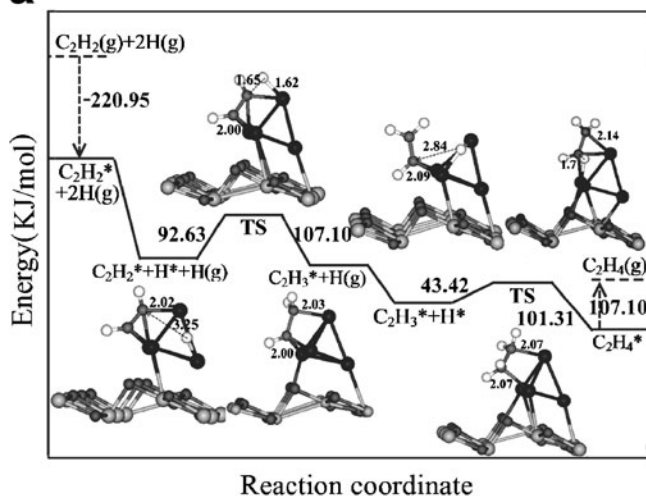
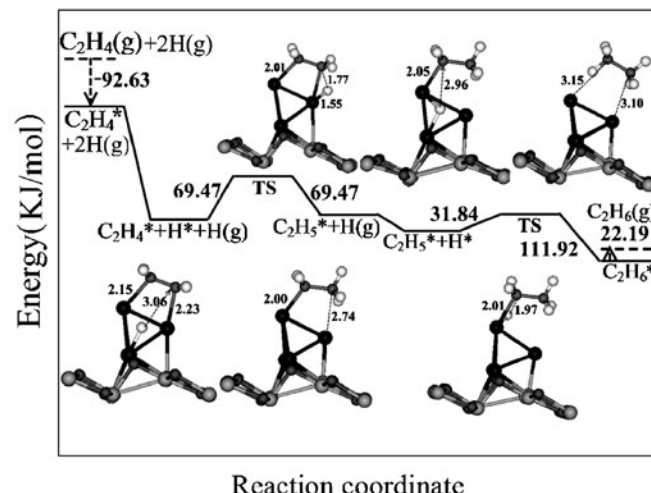
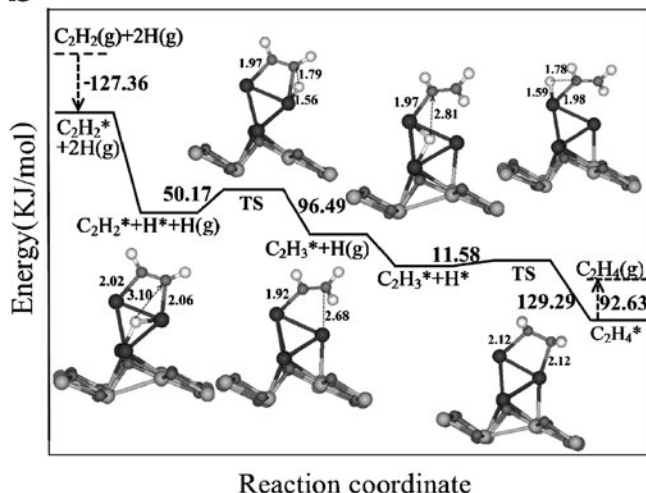
**Fig. 3** PDOS of Pd 3d states obtained at the GGA + U level on the perfect (a), defective (b) anatase  $\text{TiO}_2(101)$  surfaces supported Pd<sub>4</sub> clusters and the PDOS of isolated Pd<sub>4</sub> cluster (c)

length, for the interaction between the Pd<sub>4</sub> cluster and the supports.

In order to find out the nature of the point defect on the two anatase surfaces, the analysis of charge transfer mechanism is very necessary. Therefore, the Bader charge analysis is employed to calculate the charge distribution. For Pd<sub>4</sub> cluster adsorbed on the perfect anatase surface, there are 0.24 electrons transferring from the Pd<sub>4</sub> cluster to the titania substrate. However, it changes when oxygen deficiency exists. When Pd<sub>4</sub> is adsorbed on defective titania, electron transfer takes place to the Pd cluster from the oxide surface, which loses 0.50 electrons to the Pd<sub>4</sub> cluster. That means more charges transfer between the defective anatase substrate and Pd<sub>4</sub> cluster, thus producing an interaction effect between the metal and support and inducing Pd polarization effect. Na-Phattalung et al. [29] hold the opinion that the removal of the oxygen leaving two additional electrons will become a double donor. Namely, the removal of lattice O atoms in anatase  $\text{TiO}_2$  causes both the reduction in the material and the formation of “ $\text{Ti}^{3+}$ ” ions [22]. As for the generation of  $\text{Ti}^{3+}$ , it accepts 0.35 charges from the nearer O vacancy. Yang et al. [17] also pointed out that two excess electrons occupy the localized 3 d orbitals of the nearest-neighbor Ti. Thus we supposed that the transferred electrons are supposed to come from the previously filled Ti 3 d orbitals. Aiming to provide insight into the nature of the electrons transfer, the projected density of state (PDOS) plot of Pd<sub>4</sub> d orbitals on the perfect and defective anatase titania substrates are calculated by DFT+U method. The Fermi energy is set to be 0 eV. Compared to the PDOS of the isolated Pd<sub>4</sub> cluster displayed in Fig. 3(c), it is shown that an amount of filled Pd 3d states is much higher on the defective titania (Fig. 3(b)) and immediately below the Fermi level. When Pd cluster lying on the surface of defective titania, the substrate acts as electron donors and thus smaller band gaps exist. The electrons left in the valence band can be excited into the conduction band easily. While Pd cluster is adsorbed on the perfect titania surface (Fig. 3(a)), larger band gap exhibits as electron transfer takes place to the oxide surface from the Pd cluster. This is in accordance with the results by the Bader charge analysis.



**Fig. 4** Side views of the three binding modes ( $\pi$ , di- $\sigma$  and  $\eta_1$ - $\eta_2$  modes) of acetylene adsorbed on the Pd<sub>4</sub> cluster. Bond lengths are in Å

**a****b**

**Fig. 5** Reaction steps of acetylene hydrogenation on the perfect (a) and defective (b) anatase  $\text{TiO}_2(101)$  surfaces supported  $\text{Pd}_4$  clusters. Activation energy, reaction heat and corresponding geometry parameters of TS are pointed out. Bond lengths are in Å

### Acetylene

Acetylene adsorbs at the  $\text{Pd}_4$  cluster in three binding modes, including  $\pi$ , di- $\sigma$  and  $\eta 1\text{-}\eta 2$  modes (in Fig. 4). For perfect titania surface,  $\text{Pd}_4$  cluster constructs a tetrahedral structure, where  $\text{Pd}_4$  locates at the top site of the  $\text{Pd}_3$  triangle. When acetylene adsorbs on the clusters, the three binding modes ( $\pi$ , di- $\sigma$  and  $\eta 1\text{-}\eta 2$  modes see in Fig. 4) are considered. Their adsorption energies are  $-98.41$  and  $-220.95$   $\text{kJ mol}^{-1}$  at the  $\pi$  and  $\eta 1\text{-}\eta 2$  modes. And the di- $\sigma$  mode is less stable and transfers into the  $\eta 1\text{-}\eta 2$  mode, which bridges two  $\text{Pd}$  atoms by a single carbon atom and the other carbon atom bonds with another adjacent  $\text{Pd}$  atom at the threefold hollow site, in accordance with the proposed literature structure [30–32]. As for defective titania surface,  $\text{Pd}_4$  cluster forms a distorted tetrahedral structure occupying the oxygen vacancy site with  $\text{Pd}_2\text{-Pd}_4$  bond axis is almost parallel to the

terrace of anatase (101) surface. Here, acetylene initially binds at the three-fold hollow site and will transfer into the di- $\sigma$  mode, with the adsorption energy of  $-127.36$   $\text{kJ mol}^{-1}$ . Thus, oxygen deficiency causes different adsorbed structures of acetylene molecule, which induces the variation of adsorption energy. On perfect anatase surface, it is  $-220.95$   $\text{kJ mol}^{-1}$  with higher adsorption energy than that on the defective surface ( $-127.36$   $\text{kJ mol}^{-1}$ ). Moreover, on isolated  $\text{Pd}_4$  cluster, acetylene prefers to bind at a three-fold adsorption site in a  $\eta 1\text{-}\eta 2$  mode, which is consistent with the structure on  $\text{Pd}(111)$  surface [30, 32], and its adsorption energy is  $-223.85$   $\text{kJ mol}^{-1}$ , which is higher than that on the  $\text{TiO}_2$  surfaces. In conclusion, acetylene molecule interacts weakly with  $\text{Pd}_4$  cluster lying on the defect surface. In other words, the fact may lie in that  $\text{Pd}_4$  cluster has interaction with substrates on the defective surface.

**Table 1** Coadsorption energies and C–H distances of  $C_2H_Y + H$  system. The values of  $R_{C\text{--}H(1)}$  refer to the distance between the  $C_2H_Y$  and H; the values of  $R_{C\text{--}H(2)}$  refer to the other C–H bond lengths of the  $C_2H_Y$  system

Substrates	Species	Types	$E_{\text{ads}}$ /kJ/mol	$R_{C\text{--}M}/\text{\AA}$	$R_{H\text{--}M}/\text{\AA}$	$R_{C\text{--}H(1)}/\text{\AA}$	$R_{C\text{--}C}/\text{\AA}$	$R_{C\text{--}H(2)}/\text{\AA}$
Pd <sub>4</sub> /TiO <sub>2</sub> -perfect	$C_2H_2+H$	H: bridge	move to the threefold hollow site					
		H: threefold hollow	−436.11	2.02	1.77	3.25	1.34	1.09
		H: top	−389.80	2.02	1.61	3.29	1.35	1.09
	$C_2H_3+H$	H: bridge	−531.63	2.09	1.64	2.84	1.36	1.10
		H: threefold hollow	−529.70	2.11	1.69	3.24	1.36	1.10
		H: top	−478.57	2.06	1.52	2.87	1.36	1.10
	$C_2H_4+H$	H: bridge	move to the threefold hollow site					
		H: threefold hollow	−386.90	2.19	1.66	3.41	1.41	1.09
		H: top	−257.61	2.14	1.57	2.59	1.44	1.09
	$C_2H_5+H$	H: bridge	move to the threefold hollow site					
		H: threefold hollow	−471.81	2.06	1.73	3.47	1.50	1.10
		H: top	−394.62	2.06	1.54	3.93	1.50	1.10
Pd <sub>4</sub> /TiO <sub>2</sub> -defect	$C_2H_2+H$	H: bridge	move to the threefold hollow site					
		H: threefold hollow	−343.49	2.04	1.66	3.10	1.29	1.09
		H: top	−331.91	2.02	1.62	2.70	1.31	1.10
	$C_2H_3+H$	H: bridge	move to the threefold hollow site					
		H: threefold hollow	−448.66	1.97	1.73	2.81	1.35	1.10
		H: top	−441.90	2.00	1.66	3.68	1.37	1.10
	$C_2H_4+H$	H: bridge	move to the threefold hollow site					
		H: threefold hollow	−312.61	2.19	1.67	3.06	1.41	1.10
		H: top	−301.03	2.16	1.63	2.85	1.42	1.10
	$C_2H_5+H$	H: bridge	move to the threefold hollow site					
		H: threefold hollow	−333.84	2.05	1.69	2.96	1.52	1.10
		H: top	−318.40	2.06	1.71	4.46	1.52	1.10
Pd <sub>4</sub>	$C_2H_2+H$	H: bridge	move to the threefold hollow site					
		H: threefold hollow	−440.94	2.01	1.67	3.37	1.35	1.10
		H: top	−415.85	1.96	1.59	2.54	1.38	1.09
	$C_2H_3+H$	H: bridge	−567.33	2.12	1.68	2.76	1.37	1.09
		H: threefold hollow	−547.07	2.07	1.73	3.04	1.40	1.10
		H: top	−532.60	1.98	1.58	3.60	1.46	1.10
	$C_2H_4+H$	H: bridge	move to the threefold hollow site					
		H: threefold hollow	−394.62	2.18	1.73	3.87	1.39	1.09
		H: top	−338.66	2.18	1.70	3.21	1.39	1.09
	$C_2H_5+H$	H: bridge	−454.44	2.04	1.67	2.99	1.49	1.09
		H: threefold hollow	−471.81	2.00	1.68	3.90	1.51	1.11
		H: top	−385.94	2.14	1.62	3.67	1.49	1.09

## Vinyl

The structures of vinyl adsorbed on the Pd<sub>4</sub> clusters on the two TiO<sub>2</sub> supports are presented in Fig. 5. When it adsorbs at the isolated Pd<sub>4</sub> cluster, it binds in a  $\eta 1\text{--}\eta 2$  mode and their C–C bond length is 1.45 Å. On the perfect titania surface, it forms the same mode with the corresponding C–C bond length being 1.45 Å. However, on the defective surface it tends to adsorb in a proximate di- $\sigma$  configuration, with one C–Pd bond cleavage. And its C–C bond length is 1.34 Å,

which is shorter and presents a double bond character. It indicates that O deficiency may cause different adsorbed structures of vinyl. Besides, the adsorption energies on the isolated Pd<sub>4</sub> cluster and the perfect, defective TiO<sub>2</sub> surfaces are −303.93, −275.95 and −217.09 kJ mol<sup>−1</sup>, which shows that the interaction between the vinyl and palladium is weakened for selecting defective anatase titania as substrate. And after using the TiO<sub>2</sub> as the support, it may decrease the adsorption energies of vinyl, which mainly owes to the metal-support interaction effect.

### Ethylene

The selective hydrogenation of acetylene to ethylene is determined by two factors, which are the adsorption energies of acetylene and ethylene. Studt et al. [1] insisted that a catalyst should bind acetylene strongly and ethylene weakly to be simultaneously active and selective. Thus, the structures of ethylene are considered. On the two surfaces, ethylene molecules are likely to form the di- $\sigma$  mode on the distorted tetrahedral  $Pd_4$  cluster. However, it is likely to form a  $\pi$  mode on the isolated  $Pd_4$  cluster and its adsorption energy is  $-116.75\text{ kJ mol}^{-1}$ , in accordance with the results of  $-117.71\text{ kJ mol}^{-1}$  by Valero [25]. Compared with the adsorption energies of ethylene ( $-107.10\text{ kJ mol}^{-1}$  on perfect anatase and  $-92.63\text{ kJ mol}^{-1}$  on defect anatase), it is relatively weak and easier to desorb from the defective surface. Therefore, the defective anatase titania support has a positive effect on ethylene desorption.

### Ethyl and ethane

The unselective formation of both ethyl and ethane is caused by the over-hydrogenation of ethylene. After optimization, the ethyl molecules on the three surfaces (the isolated cluster, the perfect and defect  $TiO_2$  surface) prefer to adsorb in a proximate di- $\sigma$  configuration, with one C-Pd bond forming and the corresponding C-Pd bond length being 2.00, 2.07 and 2.00 Å. The adsorption energies of ethyl are  $-190.08$ ,  $-172.71$  and  $-148.59\text{ kJ mol}^{-1}$  on the three surfaces. The last step of ethyl hydrogenation to ethane is investigated on the three surfaces. On the isolated  $Pd_4$  cluster, the perfect and defective  $TiO_2$  surfaces, the adsorption energies of ethane are  $-30.88$ ,  $-29.91$  and  $-22.19\text{ kJ mol}^{-1}$ . It is considered to be a physical adsorption process for their weak adsorption energy.

### Coadsorption of $C_2H_2+H$ system

It is generally accepted that acetylene hydrogenation follows a sequential series of hydrogen addition reactions. Namely, acetylene reacts with hydrogen to form vinyl, ethylene, ethyl and ethane in consecutive steps. The adsorption of atomic hydrogen is investigated by placing the H atom on different surface sites of the  $Pd_4$  cluster. The surface sites of the  $Pd_4$  cluster considered are the bridge site, threefold hollow site and the top site. Bridge and threefold hollow sites are the principal hydrogen adsorption sites [33]. On the perfect  $TiO_2$  surface, the H adsorption energy is  $-325.15\text{ kJ mol}^{-1}$  on the bridge site, while it is  $-317.44\text{ kJ mol}^{-1}$  on the threefold hollow site; while it is not stable on the top site. For comparison, adsorption on the defect  $TiO_2$  surface is calculated to be  $-248.93\text{ kJ mol}^{-1}$  on the threefold hollow site, which is considered to be the most stable site. Besides, the adsorption of  $C_2H_2$  molecule and H atom at

several different sites on the three surfaces are investigated in order to determine the most stable IS for the  $C_2H_2+H$  coadsorption system. The adsorption energies and C-H distances are listed in Table 1.

### Hydrogenation reaction mechanism

Acetylene hydrogenation is a complex process, we discuss its main hydrogenation path on both the perfect and defect  $TiO_2(101)$  surfaces supported  $Pd_4$  cluster. Four elementary reaction steps ( $C_2H_2+H \rightarrow C_2H_3$ ,  $C_2H_3+H \rightarrow C_2H_4$ ,  $C_2H_4+H \rightarrow C_2H_5$  and  $C_2H_5+H \rightarrow C_2H_6$ ) are involved and calculated, which follow the Horiuti-Polanyi mechanism [34]. The most stable structures of IS, TS, FS (final states) and the details of all the intermediate are listed in Fig. 5. Initially, the acetylene molecule binds at a  $\eta 1\text{-}\eta 2$  mode at the threefold hollow site and the hydrogen atom adsorbs at the bridge site of Pd atoms. And then the hydrogen atom binds at the threefold hollow site with the C-H distance of 3.25 Å on the perfect surface. At the TS, hydrogen atom moves to sit at the nearer Pd atom with the C-H distance of 1.65 Å. However, on the defective surface, acetylene binds at the bridge site with the movement of hydrogen atom, which firstly sits at the threefold hollow site and then transfers to the top site of the nearer Pd atom. Its bond length of TS is 1.79 Å. With the increment of O deficiency, the structure effect exists. The value of activation energy on perfect anatase surface ( $92.63\text{ kJ mol}^{-1}$ ) is much higher than that on defective one ( $50.17\text{ kJ mol}^{-1}$ ), which is consistent with the adsorption energy trend of acetylene, namely the adsorption strength of acetylene on defect surface is lower than that on the perfect surface.

The product of the first hydrogenation step is vinyl, and then vinyl further hydrogenates to ethylene. The activation

**Table 2** Energy decomposition of the calculated activation energy of the first hydrogenation step (unit:  $\text{kJ mol}^{-1}$ )

	Pd <sub>4</sub> / TiO <sub>2</sub> -perfect	Pd <sub>4</sub> / TiO <sub>2</sub> -defect
$E_a$	92.63	50.17
$E_{TS}^{ads}$	-343.49	-292.35
$E_{TS}^{C2H2}$	-429.36	-281.74
$E_{TS}^H$	-181.39	-157.27
$E_{TS}^{int}$	267.26	146.66
$E_{IS}^{coads}$	-436.11	-342.52
$E_{IS}^{C2H2}$	-373.40	-213.23
$E_{IS}^H$	-257.61	-203.58
$E_{IS}^{int}$	194.90	74.29
$\Delta(\sum E_{frag})$	20.26	-22.19
$\Delta E_{int}$	72.36	72.36

energy is 43.42 kJ mol<sup>-1</sup> on the perfect anatase surface, while it is lower on the defective one (11.58 kJ mol<sup>-1</sup>). And the corresponding C-H bond lengths are 1.71 and 1.78 Å at the TS. It is obviously shown that the reaction of vinyl hydrogenation goes faster on the defective surface, which is attributed to the lower value of the activation energy. Therefore, the different structures of adsorbate caused by oxygen deficiency can also change the activity of the hydrogenation reaction.

The third hydrogenation step is ethylene hydrogenation to ethyl. It forms with the movement of the hydrogen atom from the initial position and closer to the ethylene molecule at the bridge site on the TiO<sub>2</sub> surface. Their C-H bond lengths of the TS are 1.61 and 1.77 Å. The activation energies are 82.98 and 69.47 kJ mol<sup>-1</sup> on the perfect and defective surfaces. Besides, the desorption energy of ethylene on the perfect surface is 107.10 kJ mol<sup>-1</sup>, while it is 92.63 kJ mol<sup>-1</sup> on the defective surface. Therefore, ethylene easier desorbs from defect anatase and thus may lead to the higher selectivity for the ethylene formation on the defect anatase.

And the last hydrogenation step is ethane formation, with the single C-Pd bond cleavage. The activation energy is 92.63 kJ mol<sup>-1</sup> on the perfect surface, while it is decreased to 31.84 kJ mol<sup>-1</sup> on the defective surface, with the corresponding C-H bond length 1.53 and 1.97 Å at the TS. Thus, it is obviously shown that ethyl hydrogenation is more active on the defective surface. For the lower adsorption energies of ethane on the two surfaces (−29.91 and −22.19 kJ mol<sup>-1</sup>), it is easy to desorb from the surfaces.

Through the analysis of each hydrogenation step, our results are apparently gained. Due to the oxygen deficiency, the electronic effect is significantly performed, which influences the structures of the adsorbates and the catalytic properties. On the defective surface, weaker strength exists between the Pd clusters and the adsorbed molecules, which is easier for ethylene to desorb from the Pd surface for higher selectivity. And the relative high activation energy on the perfect titania surface means a bigger barrier of acetylene to ethane, which decreased the activity of the catalyst. In a word, oxygen deficiency plays an important role in the catalytic properties in acetylene hydrogenation.

### Physical nature of the energy barrier for the first step of acetylene hydrogenation

To provide further insight into the co-adsorption effects and the nature of the reaction barrier on the first step of acetylene hydrogenation, the following scheme to decompose the calculated barrier is introduced in this work. The calculated adsorption energy of the TS ( $E_{\text{TS}}^{\text{ads}}$ ) is decomposed into  $E_{\text{TS}}^{\text{C2H2}}$

and  $E_{\text{TS}}^{\text{H}}$  as following formula:  $E_{\text{TS}}^{\text{ads}} = E_{\text{TS}}^{\text{C2H2}} + E_{\text{TS}}^{\text{H}} + E_{\text{TS}}^{\text{int}}$  [35, 36]. Here  $E_{\text{TS}}^{\text{C2H2}}$ ,  $E_{\text{TS}}^{\text{H}}$  and  $E_{\text{TS}}^{\text{int}}$  are the rebonding energy of C<sub>2</sub>H<sub>2</sub> fragment, H fragment and the interaction between the two fragments. A similar decomposition is gained for the coadsorption energy of IS ( $E_{\text{IS}}^{\text{coads}}$ ) by the formula:  $E_{\text{IS}}^{\text{coads}} = E_{\text{IS}}^{\text{C2H2}} + E_{\text{IS}}^{\text{H}} + E_{\text{IS}}^{\text{int}}$ . Here  $E_{\text{IS}}^{\text{C2H2}}$ ,  $E_{\text{IS}}^{\text{H}}$  and  $E_{\text{IS}}^{\text{int}}$  are the adsorption energies of C<sub>2</sub>H<sub>2</sub> fragment, H fragment and the interaction energy at the IS. Therefore, the activation energy  $E_a$  is divided as a function of the variations of both the rebonding and adsorption energy summed over the fragments  $\Delta(\sum E_{\text{frag}})$  and the variations of the interaction energy ( $\Delta E_{\text{int}}$ ), between the IS and the TS. Then the formula is  $E_a = E_{\text{TS}}^{\text{ads}} - E_{\text{IS}}^{\text{coads}} = \Delta(\sum E_{\text{frag}}) + \Delta E_{\text{int}}$ .

We display the contributions to the energy barrier of each term for the first hydrogenation step (acetylene hydrogenation to vinyl) in Table 2. As can be seen, one can find that the interaction energy ( $\Delta E_{\text{int}}$ ) has the same value of 72.36 kJ mol<sup>-1</sup> on both the perfect and defective surfaces, and thus the main contribution to the energy barrier comes from the sum of rebonding and adsorption energy ( $\Delta(\sum E_{\text{frag}})$ ) on these two model catalysts (*i.e.*, from 20.26 kJ mol<sup>-1</sup> on perfect and −22.19 kJ mol<sup>-1</sup> on oxygen defect anatase TiO<sub>2</sub>(101) as seen in Table 2). By careful examination of  $\Delta(\sum E_{\text{frag}})$ , we notice that the variation energy of C<sub>2</sub>H<sub>2</sub> fragment at the IS and TS exhibits a similar destabilization on the perfect and defective surfaces. That is, it is destabilized by 55.96 kJ mol<sup>-1</sup> on the perfect one (from −429.36 kJ mol<sup>-1</sup> at IS to −373.40 kJ mol<sup>-1</sup> at TS) and 68.51 kJ mol<sup>-1</sup> on the defect one (from −281.74 to −213.23 kJ mol<sup>-1</sup>), which induces a 12.55 kJ mol<sup>-1</sup> increment. On the other hand, the variation energy of H fragment is relatively large, *i.e.*, it is decreased by 76.22 kJ mol<sup>-1</sup> (from −257.61 to −181.39 kJ mol<sup>-1</sup>) on the perfect surface and 46.31 kJ mol<sup>-1</sup> (from −203.58 to −157.27 kJ mol<sup>-1</sup>) on the defective surface from the IS and TS. More variation exists in H fragment, which can be further confirmed by the transition state analysis. The H atom moves from the threefold hollow at IS to the top site at TS with the C-Pd bond length of 1.62 Å; while it transfers from the threefold hollow site to the top site at TS with the C-Pd bond length of 1.56 Å on the defective surface. Since the C-Pd bond length of TS on perfect surface is larger than on defect one, and a larger energy cost for H atom on the perfect TiO<sub>2</sub>(101) may be expected. Therefore one may conclude that the reduction of the barrier on the defect TiO<sub>2</sub>(101) is primarily affected by the low energy cost of the H fragment.

### Conclusions

In the present study, the acetylene hydrogenation on both the perfect and oxygen defective anatase TiO<sub>2</sub>(101) supported Pd<sub>4</sub> cluster has been explored by DFT+U

calculations. Our results show that the metal-support interaction effect is significantly performed solely on the defect surface instead of the perfect surface. Moreover, the results indicated that the catalytic activity of acetylene hydrogenation on oxygen defect surface is much higher than on the perfect one. The possible reasons may due to two facts: the weaker adsorption of ethylene and the lower energy barrier for the hydrogenation steps on oxygen defect surface. In conclusion, oxygen deficiency changes the catalytic properties of acetylene hydrogenation.

**Acknowledgments** This work was supported by the National Natural Science Foundation of China (Grants No. 20273034, 20673063) and the Tianhe-1 supercomputer in Tianjin.

## References

1. Stuđt F, Abild-Pedersen F, Bligaard T, Sørensen RZ, Christensen CH, Nørskov JK (2008) On the role of surface modifications of palladium catalysts in the selective hydrogenation of acetylene. *Angew Chem Int Edn* 48:9299–9302. doi:10.1002/anie.200802844
2. Panpranot J, Kontapakdee K, Praserthdam P (2006) Selective hydrogenation of acetylene in excess ethylene on micron-sized and nanocrystalline  $\text{TiO}_2$  supported Pd catalysts. *Appl Cat A General* 314:128–133. doi:10.1016/j.apcata.2006.08.024
3. Diebold U (2003) The surface science of titanium dioxide. *Surf Sci Rep* 48:53–229. doi:10.1016/S0167-5729(02)00100-0
4. Berger T, Sterrer M, Diwald O, Knözinger E, Panayotov D, Thompson TL, Yates JT (2005) Light-induced charge separation in anatase  $\text{TiO}_2$  particles. *J Phys Chem B* 109:6061–6068. doi:10.1021/jp0404293
5. Ganduglia-Pirovano MV, Hofmann A, Sauer J (2007) Oxygen vacancies in transition metal and rare earth oxides: current state of understanding and remaining challenges. *Surf Sci Rep* 62:219–270. doi:10.1016/j.surrep.2007.03.002
6. Panpranot J, Kontapakdee K, Praserthdam P (2006) Effect of  $\text{TiO}_2$  crystalline phase composition on the physicochemical and catalytic properties of Pd/ $\text{TiO}_2$  in selective acetylene hydrogenation. *J Phys Chem B* 110:8019–8024. doi:10.1021/jp057395z
7. Mekasuwandumrong O, Phothakwanpracha S, Jongsomjit B, Shotipruk A, Panpranot J (2010) Liquid-phase selective hydrogenation of 1-Heptyne over Pd/ $\text{TiO}_2$  catalyst synthesized by one-step flame spray pyrolysis. *Catal Lett* 136:164–170. doi:10.1007/s10562-010-0313-4
8. Yin H, Wada Y, Kitamura T, Kambe S, Murasawa S, Mori H, Sakata T, Yanagida S (2001) Hydrothermal synthesis of nanosized anatase and rutile  $\text{TiO}_2$  using amorphous phase  $\text{TiO}_2$ . *J Mater Chem* 11:1694–1703. doi:10.1039/b008974p
9. Li Y, Xu B, Fan Y, Feng N, Qiu A, He JMJ, Yang H, Chen Y (2004) The effect of titania polymorph on the strong metal-support interaction of Pd/ $\text{TiO}_2$  catalysts and their application in the liquid phase selective hydrogenation of long chain alkadienes. *J Mol Catal A* 216:107–114. doi:10.1016/j.molcata.2004.02.007
10. Xu C, Lai X, Zajac GW, Goodman DW (1997) Scanning tunneling microscopy studies of the  $\text{TiO}_2(110)$  surface: structure and the nucleation growth of Pd. *Phys Rev B* 56:13464–13482. doi:10.1103/PhysRevB.56.13464
11. Zhang J, Zhang M, Han Y, Li W, Meng X, Zong B (2008) Nucleation and growth of palladium clusters on anatase  $\text{TiO}_2(101)$  surface: a first principle study. *J Phys Chem C* 112:19506–19515. doi:10.1021/jp8036523
12. Kresse G, Furthmüller J (1996) Efficiency of ab-initio total energy calculations for metals and semiconductors using a plane-wave basis set. *Comput Mater Sci* 6:15–50. doi:10.1016/0927-0256(96)00008-0
13. Kresse G, Furthmüller J (1996) Efficient iterative schemes for *ab initio* total-energy calculations using a plane-wave basis set. *Phys Rev B* 54:11169–11186. doi:10.1103/PhysRevB.54.11169
14. Perdew JP, Wang Y (1992) Accurate and simple analytic representation of the electron-gas correlation energy. *Phys Rev B* 45:13244–13249. doi:10.1103/PhysRevB.45.13244
15. Blöchl PE (1994) Projector augmented-wave method. *Phys Rev B* 50:17953. doi:10.1103/PhysRevB.50.17953
16. Kresse G, Joubert D (1999) From ultrasoft pseudopotentials to the projector augmented-wave method. *Phys Rev B* 59:1758. doi:10.1103/PhysRevB.59.1758
17. Yang K, Dai Y, Huang B, Feng YP (2010) Density-functional characterization of antiferromagnetism in oxygen-deficient anatase and rutile  $\text{TiO}_2$ . *Phys Rev B* 81:033202. doi:10.1103/PhysRevB.81.033202
18. Islam MM, Calatayud M, Pacchioni G (2011) Hydrogen adsorption and diffusion on the anatase  $\text{TiO}_2(101)$  surface: a first-principles investigation. *J Phys Chem C* 115:6809–6814. doi:10.1021/jp200408v
19. Yin XL, Calatayud M, Qiu H, Wang Y, Birkner A, Minot C, Wöll C (2008) Diffusion versus desorption: complex behavior of H atoms on an oxide surface. *ChemPhysChem* 9:253–256. doi:10.1002/cphc.200700612
20. Han G-b, Hu S-j, Yan S-s, Mei L-m (2009) Oxygen vacancy induced ferromagnetism in rutile  $\text{TiO}_{2-x}$ . *Phys Status Solidi RRL* 3:148–150. doi:10.1002/pssr.200903078
21. Finazzi E, Di Valentin C, Pacchioni G, Selloni A (2008) Excess electron states in reduced bulk anatase  $\text{TiO}_2$ : comparison of standard GGA, GGA + U, and hybrid DFT calculations. *J Chem Phys* 129:154113–154119. doi:10.1063/1.2996362
22. Mills G, Jónsson H, Schenter GK (1995) Reversible work transition state theory: application to dissociative adsorption of hydrogen. *Surf Sci* 324:305–337. doi:10.1016/0039-6028(94)00731-4
23. Monkhorst HJ, Pack JD (1976) Special points for Brillouin-zone integrations. *Phys Rev B* 13:5188. doi:10.1103/PhysRevB.13.5188
24. Pan Y-x, Liu C-j, Ge Q (2010) Effect of surface hydroxyls on selective  $\text{CO}_2$  hydrogenation over  $\text{Ni}_4/\gamma\text{-Al}_2\text{O}_3$ : a density functional theory study. *J Catal* 272:227–234. doi:10.1016/j.jcat.2010.04.003
25. Valero MC, Raybaud P, Sautet P (2007) Interplay between molecular adsorption and metal-support interaction for small supported metal clusters: CO and  $\text{C}_2\text{H}_4$  adsorption on  $\text{Pd}_4/\gamma\text{-Al}_2\text{O}_3$ . *J Catal* 247:339–355. doi:10.1016/j.jcat.2007.02.014
26. Sanz JF, Márquez A (2007) Adsorption of Pd atoms and dimers on the  $\text{TiO}_2(110)$  surface: a first principles study. *J Phys Chem C* 111:3949–3955. doi:10.1021/jp801591z
27. Zácarias AG, Castro M, Tour JM, Seminario JM (1999) Lowest energy states of small Pd clusters using density functional theory and standard *ab Initio* methods. A route to understanding metallic nanoprobes. *J Phys Chem A* 103:7692–7700. doi:10.1021/jp9913160
28. Valero MC, Raybaud P, Sautet P (2007) Nucleation of  $\text{Pdn}$  ( $n=1-5$ ) clusters and wetting of Pd particles on  $\gamma\text{-Al}_2\text{O}_3$  surfaces: a density functional theory study. *Phys Rev B* 75:045427. doi:10.1103/PhysRevB.75.045427
29. Na-Phattalung S, Smith MF, Kim K, Du M-H, Wei S-H, Zhang SB, Limpijumpong S (2006) First-principles study of native defects in anatase  $\text{TiO}_2$ . *Phys Rev B* 73:125205. doi:10.1103/PhysRevB.73.125205
30. Sellers H (1990) Structures and vibrational frequencies of acetylene in three binding sites on the palladium(111) surface. *J Phys Chem* 94:8329–8333. doi:10.1021/j100384a061

31. Lee L-Q, Cao P-L (1996) Acetylene adsorption studies on Pd(111) and stepped Pd(111). *J Phys Condens Matter* 8:3313–3322. doi:[10.1088/0953-8984/8/19/007](https://doi.org/10.1088/0953-8984/8/19/007)
32. Sheth PA, Neurock M, Smith CM (2003) A first-principles analysis of acetylene hydrogenation over Pd(111). *J Phys Chem B* 107:2009–2017. doi:[10.1021/jp021342p](https://doi.org/10.1021/jp021342p)
33. Bertin V, Cruz A, Del Angel G, Castro M, Poulain E (2005) The H and H<sub>2</sub> interaction with Pd<sub>3</sub>Cu, Pd<sub>4</sub>, and Cu<sub>4</sub> fcc (111) clusters: a DFT comparative study. *Int J Quantum Chem* 102:1092–1105. doi:[10.1002/qua.20426](https://doi.org/10.1002/qua.20426)
34. Mei D, Sheth PA, Neurock M, Smith CM (2006) First-principles-based kinetic Monte Carlo simulation of the selective hydrogenation of acetylene over Pd(111). *J Catal* 242:1–15. doi:[10.1016/j.jcat.2006.05.009](https://doi.org/10.1016/j.jcat.2006.05.009)
35. Dupont C, Jugnet Y, Loffreda D (2006) Theoretical evidence of PtSn alloy efficiency for CO oxidation. *J Am Chem Soc* 128:9129–9136. doi:[10.1021/ja061303h](https://doi.org/10.1021/ja061303h)
36. Hammer B (2000) Adsorption, diffusion, and dissociation of NO, N and O on flat and stepped Ru(0001). *Surf Sci* 459:323–348. doi:[10.1016/S0039-6028\(00\)00467-2](https://doi.org/10.1016/S0039-6028(00)00467-2)